Measurements of the Turbulence in an Abyssal Boundary Layer

A. J. ELLIOTT[1]

Institute of Oceanographic Sciences, Wormley, Godalming, Surrey, GU8 5UB, U.K.

(Manuscript received 11 June 1984, in final form 6 September 1984)

ABSTRACT

Electromagnetic sensors have been used to measure the turbulent current fluctuations 50 cm above the sea bed at a depth exceeding 4000 m on an abyssal plain. Bursts of turbulent energy typically lasted for about 50 s and showed a peak instantaneous $-uw$ perturbation product of about 0.25 cm^2 s^{-2}. The horizontal and vertical integral length scales were estimated to be around 150 and 30 cm, respectively, in a mean flow of about 3 cm s^{-1}. The eddy correlation method gave estimates for the friction velocity of around 0.12 cm s^{-1} and the bottom drag coefficient was estimated to be 1.9×10^{-3}. When normalized by variance, height above bottom and wave number the spectra agree with the similarity scaling suggested by Soulsby, and the statistics of the turbulence are consistent with existing results obtained from atmospheric and shallow water boundary layers.

1. Introduction

As part of a study into the properties and dynamics of the benthic boundary layer, an electromagnetic current meter system has been developed to obtain near-bottom estimates of the vertical momentum flux (Fig. 1). It is planned that the instrument will be used in the future with conventional instruments, such as moored current meter arrays and neutrally buoyant floats, to investigate mixing within the benthic boundary layer and its relation to the dynamical forcing of the overlying water. Observations of the boundary layer in the western North Atlantic (Armi and Millard, 1976; D'Asaro, 1982) suggested that the thickness of the benthic boundary layer was related to the mean advective speed of the overlying water, although the observed layers were several times thicker than the expected Ekman layer thickness. More recently, modeling studies (Richards, 1984) have suggested that the thickness of the boundary layer may be controlled by the convergence and divergence of the flow induced by mesoscale eddies in the overlying water and that frictional effects may be of only secondary importance. The goal of the present instrumental program is to measure the near-bottom turbulent stress in the eastern North Atlantic over a period of several days simultaneous to measurements of the characteristics of the benthic boundary layer and of the mesoscale flow in the overlying water, and to resolve the role played by frictional effects in the development of the boundary layer. There are similar projects (for example, Weatherly and Wimbush, 1980) that are aimed at understanding the dynamics of the boundary layer in the western North Atlantic. The present results are concerned with an evaluation of the electromagnetic current sensors at abyssal depths and with preliminary estimates of the near-bottom shear stress.

The electromagnetic heads sampled once per second for 20 minutes every 3 hours at a height 50 cm above the sea bed, while a mechanical rotor and vane sampled continuously every 20 s to provide a check on zero drift. At the start and end of each 20-minute sampling period there was a 20-second calibration check during whch the tilt and orientation of the framework were recorded. The electromagnetic heads are annular in design and have a diameter of 15 cm, their output representing a velocity with a spatial averaging width of about 10 cm (Collar and Griffiths, 1980). Each head measures the horizontal and vertical component of the flow across its face; by arranging two heads perpendicular to each other both horizontal components, u and v, and two estimates of the vertical flow, w and w', were obtained. The two heads were separated horizontally by about 50 cm, and their circuitry was designed to cover a speed range of ± 40 cm s^{-1} with a logger resolution of about 0.02 cm s^{-1}. They were calibrated in a tow tank over speeds of 0–8 cm s^{-1} (the expected abyssal range) and showed a linear and repeatable response; currents determined by the heads should have a relative accuracy to better than 0.1 cm s^{-1}. A Savonius rotor was used to check on the zero drift of the heads and to enable the absolute velocities to be determined. Unfortunately, the rotor was not accurate at low speed because of variability in its threshold caused

[1] Present affiliation: Unit for Coastal and Estuarine Studies, Marine Science Laboratories, Menai Bridge, Anglesey, LL59 5EY, U.K.

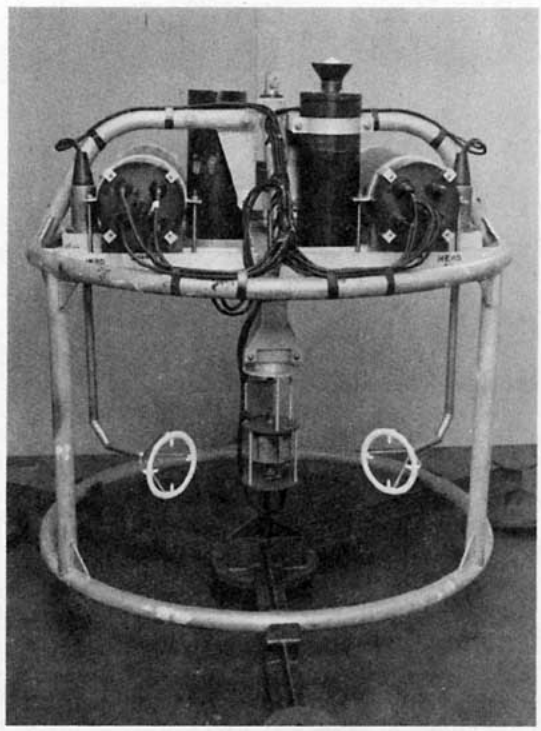

FIG. 1. The experimental rig showing the electromagnetic sensors, the electronics pressure housings and the protective cage with anchor base. The mechanical rotor and vane assembly is at the center of the cage.

by friction in the bearings. During tests in a tow tank the threshold varied between 1.2 and 1.8 cm s^{-1} and the rotor count showed variations of up to 10% at speeds of around 5 cm s^{-1}. Thus the rotor output cannot be considered to be more accurate than 0.5 cm s^{-1}. A mechanical vane was used to obtain the flow direction and this had a logger resolution of about 0.2°; however, this was also affected by friction at low speed and the vane output was probably only accurate to about 10°. The tilt of the framework, sampled at the start and end of each 20-minute recording period, was considered to be accurate to better than 0.1°. The data were recorded onto a digital logger, each 16-bit data word being composed of a 4-bit channel identifier and a 12-bit data string. With a 20-minute sampling interval every 3 hours the logger had a capacity to store about 7 days of data, representing about 10^5 data cycles which, after decoding, produces around 2×10^6 data words.

The sensors were surrounded by a protective cage which sat on an anchor base (Fig. 1). The base was released by acoustic command and the package recovered using buoyancy spheres attached to the top of the frame. The test deployment was made during February 1983 at 40°23.7′N, 20°34.4′W (Fig. 2). The site was about 550 km northeast of the Azores on the edge of the Iberian Abyssal Plain where water depth was around 4270 m. The depth decreased

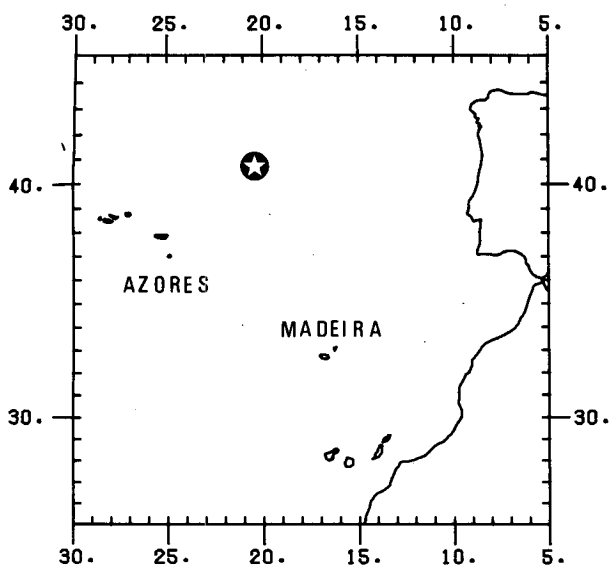

FIG. 2. The measurement site located 550 km to the northeast of the Azores.

northwest of the site in relation to the ridge of the Azores–Biscay Rise which runs towards the northeast and rises to a height of about 600 m relative to the test site (Fig. 3). Topography to the east of the site is comparatively flat, although there are two small hills, each about 700 m high, 40 km to the west and southwest of the site. Echo-sounding profiles of the test site showed the area to be relatively flat with topographic variations of about 20 m occurring on scales of about 1 km; thus the local slope is less than 2°. The sea bed in this area is a calcareous ooze composed of about 50% clay, 25% silt and 25% sand (R. B. Kidd, personal communication, 1984). No

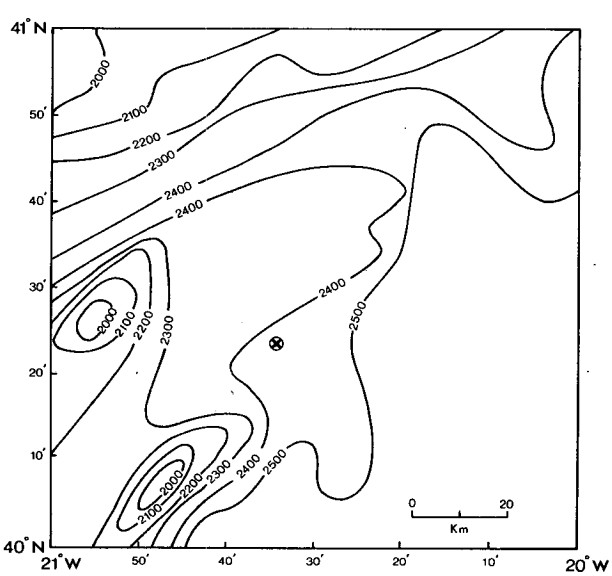

FIG. 3. General bathymetry of the area; depth contours are in fathoms (1 fathom = 1.83 m).

photographs were taken of the sea floor; however, evidence has been found 50 km to the northwest of small scale features 5–10 cm in diameter and 1–2 cm high (Q. Huggett, personal communication, 1984) that are likely to be caused by bioturbation. These are comparable to features observed on the Madeira Abyssal Plain (Elliott and Thorpe, 1983) and suggest that similar features exist at the site of the turbulence measurements. The instrument was launched on 7 February and recovered on 16 February; a total of fifty 20-minute runs were recorded on the sea bed before the logger capacity was exceeded on 13 February.

No deep CTD measurements were made during the cruise, so no information is available on the thickness and character of the benthic boundary layer. However, temperature measurements made at comparable depths on the Madeira Abyssal Plain (Saunders, 1983) have shown the benthic boundary layer to have a thickness of 10–30 m and it is reasonable to expect a similar thickness at the test site.

The flow measured by the heads was unobstructed by the framework for a range of approach angles covering about 130°. Runs must be rejected from the analysis when the flow reaches the heads from the sides or back of the frame. Measurements of the near-bottom flow on the Madeira Abyssal Plain (Elliott and Thorpe, 1983) indicate that the flow is oscillatory in character because of the strength of the inertial and tidal components; thus it was expected that about one-third of the runs would occur during conditions of unobstructed flow.

2. Results

After free-falling from the surface the framework was orientated on the sea bed with the current sensors towards the west, the instrument tilting down towards the northwest at a fixed angle of less than 2°. The mechanical vane was damaged during launch of the instrument and did not respond to the flow; therefore the zero offsets of the electromagnetic heads were determined by matching the mean speeds over each of the 20-minute runs between the rotor and the current heads for those runs when the rotor was not stalled. This gave a series of 31 pairs of speed values that could be matched by least squares. (A comparison between speeds determined from rotor count and from vector-mean components is valid since the steadiness of the flow in the benthic boundary layer should be greater than 0.95 during periods of 20 minutes.) After correction for zero offset, the speed determined by the electromagnetic heads agreed with the non-stalled rotor speed to generally better than 0.2 cm s^{-1}, except for the final runs when the difference reached 1 cm s^{-1} (Fig. 4). This suggests that there may have been continuous zero-drift, but it may also have been caused by sticking of the rotor which stalled more frequently near the end of the measurements. Tests in a tow tank and in shallow water have suggested that the offsets should be stable to within 0.1 cm s^{-1} over several days. The 6-day record of current speed showed a marked tidal signal and maximum speeds that reached 5–6 cm s^{-1}. The current components were averaged over the entire record, and an estimate of 1.5 cm s^{-1} towards the

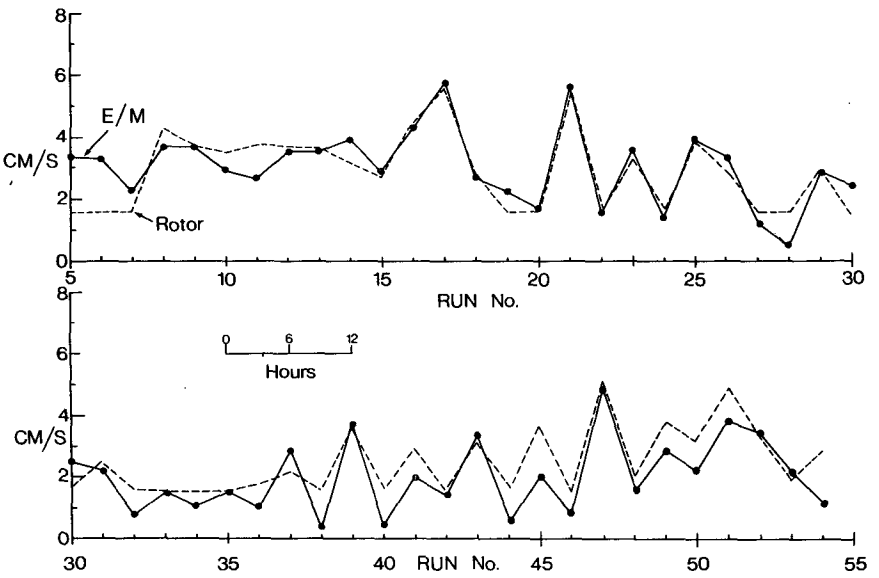

FIG. 4. Comparison of the speed determined by the rotor and from the electromagnetic heads after correction for offset; the rotor threshold was 1.8 cm s^{-1} and the corrections applied to the heads were $u_0 = 2.2$, $v_0 = -5.2$ cm s^{-1}.

south was obtained for the mean flow. The residual flow was subtracted from the data and the resulting mean tidal vectors plotted. This showed the semidiurnal tide to be directed northeastward with an amplitude of about 3 cm s^{-1}; the phase of the current along this direction was estimated to be around 40°. The M_2 surface (elevation) tide in this region has a phase of about 75° (Cartwright *et al.*, 1980); therefore, the benthic current led the surface tide by about 1.2 hours, similar to the phase difference found on the Madeira Abyssal Plain (Elliott and Thorpe, 1983). The resultant of these tidal and residual flows would thus be predominantly from the northeast which was consistent with the direction sensed by the heads. Only seven of the 50 runs were from directions when the flow was unobstructed by the framework of the instrument, these occurred when the flow was from the northwest and it was then approximately aligned with the u-velocity head.

A series of very regular fluctuations caused by eddy shedding were revealed by the current records when the flow passed through the framework before reaching the heads. Although such records could not be used to estimate bottom stress, they were useful for checking the performance of the electromagnetic heads since a knowledge of the geometry of the framework and the observed periodicity of the eddies could be used to estimate the direction and speed of the ambient flow. This could then be used as an independent check on the head zero-offsets and gave values that were comparable with those obtained by matching to the rotor speed.

The data from Run 6 were representative of the unobstructed runs and will be used to illustrate the character of benthic turbulence. Figure 5 shows the horizontal and vertical velocity components and the fluctuation product series uw and vw' from Run 6. (The 20-minute means were removed from the velocity series before calculating the cross-products, w and w' were taken as the velocities normal to the bottom and offsets were determined so that $\bar{w} = \bar{w}' = 0$.) The mean flow had components given by $\bar{u} = 3.24$ and $\bar{v} = -0.79$ cm s^{-1}. In x–y coordinates, the mean flow was directed along a bearing of $\theta = -14°$ where θ is the angle that the flow makes with the x-axis. Thus x was approximately in the direction of flow and y was transverse to it. Several events can be seen in the uw product series; those that occurred around 380–520 s after the start of the run (each lasted for about 50 s) are examples of sweeps (an increase in u associated with downward moving fluid). The events at times 600–650 s and 850–900 s are examples of ejections, when a decrease in u is associated with upward moving fluid. The striking feature of the events is their relatively long duration of about 50 s, which is an order of magnitude longer than the duration of bursts of turbulence observed in shallow water (Heathershaw, 1979) where the advective flow is much stronger. Since the speed of advective flow was around 3 cm s^{-1}, this time scale suggests that the turbulent billows had a horizontal scale of about 150 cm. The peak instantaneous value of the uw product during the 20-minute run shown in Fig. 5 had a value of about -0.25 cm^2 s^{-2} and the value of stress

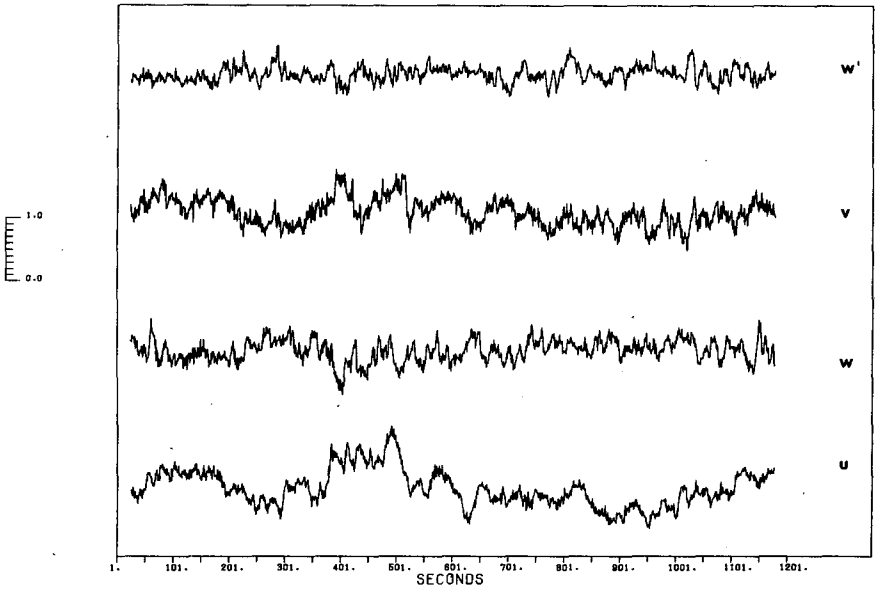

FIG. 5a. One second values of horizontal and vertical velocities during Run 6, the mean values for u and v were 3.3 and -0.8 cm s^{-1}, respectively; the vertical scale represents 1.0 cm s^{-1} (arbitrary origin).

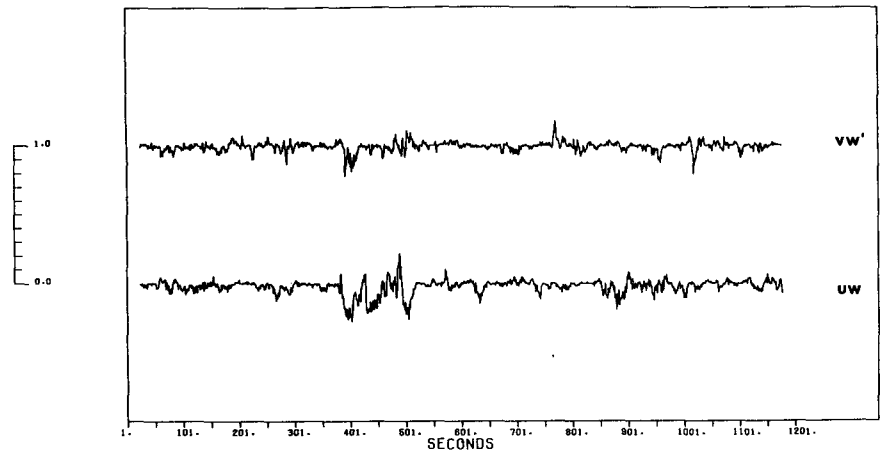

FIG. 5b. Cross-product time series of the horizontal and vertical fluctuations, uw and vw', for Run 6; the vertical scale represents 1.0 cm^2 s^{-2}.

obtained by averaging over the record length was around 0.022 dyn cm^{-2}.

Some statistics of the runs when the flow was unobstructed are given in Table 1. For all seven runs the mean flow was aligned at an angle less than 20° to the x-axis, thus $-\overline{uw}$ and $-\overline{vw}'$ are approximately the longitudinal and lateral components of stress. It is encouraging that all of the estimates of $\overline{uw}$ have the correct sign for bottom generated turbulence. The ratios of fluctuations to the mean flow have been evaluated for shallow water turbulence (Bowden, 1962; Heathershaw, 1979), and for comparison the corresponding values and their mean values for the present data are shown in Table 1. Good agreement was found with the ratios obtained for shallow water flow, but it should be noted that some of these ratios are depth-dependent (since the mean flow varies logarithmically with height). If u_* is calculated from $(-\overline{uw})^{1/2}$, then the ratios σ_u/u_*, σ_v/u_* and σ_w/u_* are estimated to have values of 2.35 ± 0.14, 1.75 ± 0.14 and 1.37 ± 0.06 (error bars throughout give the standard error of the mean), respectively, which is comparable with the expected values of 2.4, 1.9 and 1.2 (Soulsby, 1983); these ratios are not height-dependent.

If the bottom stress is represented by a quadratic relationship of the form $\tau = \rho C_{50} u|u|$ and $\tau = -\rho\overline{uw}$ (assuming the flow to be purely in the x-direction), then the drag coefficient C_{50} can be estimated. The benthic data give $C_{50} = (1.89 \pm 0.43) \times 10^{-3}$. The friction velocity, $u_* = (\tau/\rho)^{1/2}$, can be estimated from Table 1 to have a value of $u_* = 0.12 \pm 0.02$ cm s^{-1}, and hence the roughness length, z_0, which if the flow is hydrodynamically smooth is given by $z_0 = 0.1\nu/u_*$, had a mean value of 0.015 ± 0.002 cm ($\nu = 1.6 \times 10^{-2}$).

Estimates of time and length scales can be obtained by integrating the autocorrelation function of a velocity series to obtain an integral time scale, and a length scale can then be obtained by multiplying by the mean advection speed. The integral time scales T_u, T_v and T_w had values of 56.2 ± 3.6, 30.6 ± 4.0 and 12.4 ± 2.8 s, respectively, with associated horizontal length scales of 164.9 ± 16.6, 91.6 ± 13.1 and 33.9 ± 5.8 cm. The ratios of the length scales L_u/L_v and L_u/L_w had values of 2.1 ± 0.3 and 6.5 ± 1.4, while the advective flow $\bar{u}$ had a mean value of 3.0 ± 0.3 cm s^{-1}. The horizontal length scale of the vertical motions was around 35 cm, comparable to

TABLE 1. Statistics of the flow, $U = (\bar{u}^2 + \bar{v}^2)^{1/2}$ and $\theta = \arctan(\bar{v}/\bar{u})$, s and k are the skewness and kurtosis of the uw fluctuation product series; $r_{u,w}$ is the correlation between the horizontal and vertical components of flow. Velocity units are cm s^{-1}.

Run	$\bar{u}$	$\bar{v}$	θ	$\overline{uw}$	$\overline{vw}'$	$r_{u,w}$	$\frac{\sigma_u}{U}$	$\frac{\sigma_w}{U}$	$\frac{\sigma_w}{\sigma_u}$	s	k
6	3.3	−0.8	−14	−0.021	−0.007	−0.46	0.08	0.05	0.65	−1.6	8.0
23	3.4	−1.0	−17	−0.020	−0.001	−0.40	0.09	0.02	0.56	−2.6	13.4
31	2.2	0.0	0	−0.006	0.000	−0.23	0.11	0.05	0.42	−1.3	6.7
39	3.7	−0.2	−3	−0.012	−0.002	−0.27	0.07	0.05	0.62	−1.2	8.5
43	3.3	−0.4	−7	−0.007	−0.001	−0.33	0.05	0.04	0.73	−1.5	7.9
48	1.5	0.5	19	−0.007	−0.000	−0.26	0.14	0.08	0.60	−0.6	4.5
52	3.4	−0.8	−13	−0.043	−0.019	−0.39	0.13	0.07	0.57	−1.6	7.5
Mean						−0.33	0.10	0.05	0.59	−1.5	8.1

the height of the sensors above the sea bed (50 cm) which suggests that the vertical billows were limited by their elevation above the sea floor.

Figure 6 shows the spectra of the horizontal and vertical velocity series (u and w) from Run 6. Each record was broken into two pieces each 512 s long and adjacent spectral estimates averaged within each block before results from the two blocks were combined. The spectra show a high-frequency tail, with a spectral level of around 10^{-2} cm^2 s^{-1}, at time scales shorter than about 4 s. This level corresponds to a velocity fluctuation of about 0.01 cm s^{-1}, half the logger resolution value of 0.02 cm s^{-1}, suggesting that the tail is due to the logger discrimination level and aliasing. Inspection of high resolution plots of the velocity data reveals the individual logger counts and suggests that the sensors were limited by logger resolution and not by instrumental noise. Since the noise appeared at time scales shorter than 5 s, it was well separated from the time scales at which the stress-generating events occurred.

For isotropic turbulence the spectral density and the wavenumber are related by

$$E(k) = \alpha\epsilon^{2/3}k^{-5/3} \tag{1}$$

for wavenumbers within the inertial subrange (Wimbush and Munk, 1970). The turbulence will only be isotropic for wavenumbers much greater than z^{-1} where z is the height above the bottom, and for wavenumbers lower than L_k^{-1} where L_k is the Kolmogoroff fine scale, $(\nu^3/\epsilon)^{1/4}$, which can be expected to have a value of about 4 cm. In both of these expressions ϵ is the dissipation rate which can be estimated from

$$\epsilon = \frac{u_*^3}{\kappa z} \tag{2}$$

within the constant stress layer. Combining (1) and (2), and rewriting in terms of the frequency spectrum we obtain

$$E(f) = \alpha(\bar{u}/\kappa z)^{2/3}u_*^2 f^{-5/3} \tag{3}$$

where $\alpha = 0.135$, $\kappa = 0.40$ and $z = 50$ cm. The constant stress layer has a thickness of $0.2C_D^{1/2}u_*/f_c$ where f_c is the Coriolis parameter (9.41×10^{-5}); typical values predict a layer thickness of order 10 cm if we use C_{50} as an estimate of C_D. Therefore, expression (3) may not be valid at the sensor height. Lines with a slope of $-5/3$ were fitted by least squares to each of the frequency spectra for frequencies less than 0.25 s^{-1}, i.e., neglecting the high-frequency tail, and a mean value for u_* of 0.09 ± 0.01 was obtained using (3). Values of u_* obtained by the eddy correlation method were larger by a mean factor of 1.4, and the discrepancy is probably due to the use of (2) at a height that was above the constant-stress layer. In the discussion that follows, values used for u_* were obtained by the eddy correlation method.

If the velocity profile is logarithmic then the roughness length can be estimated from

$$u = (u_*/\kappa)\ln(z/z_0),$$

which gave $z_0 = 0.016 \pm 0.01$ cm. A value for z_0 of 0.015 cm was obtained earlier by assuming that the flow was hydrodynamically smooth, an assumption that is supported by the good agreement between the two values. The dissipation rate in the constant stress part of the logarithmic layer is given by $\epsilon = u_*^3/\kappa z$ and this is estimated to have a value of $(1.3 \pm 0.6) \times 10^{-4}$ cm^2 s^{-3}, although this result may not be strictly valid as noted above.

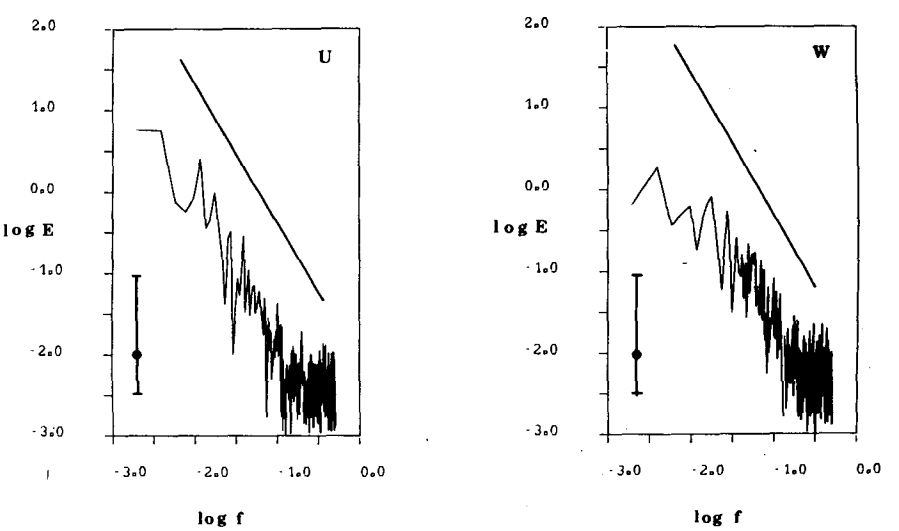

FIG. 6. Energy-density spectra versus frequency for u and w, Run 6. A $-5/3$ slope and the 95% confidence intervals are indicated.

The relative levels of the horizontal and vertical spectra were found by fitting least-squares lines with slopes of $-5/3$ to each of the spectra and comparing the intercept values. This gave an estimate for the ratio of $E_w(f)/E_u(f)$ as 1.40 ± 0.09 which can be compared with the values of 1.33 found by Heathershaw (1979) and 1.44 reported by Bowden and Ferguson (1980). Consequently, spectral levels from the benthic data were consistent with the known properties of bottom turbulence.

Soulsby (1977) has shown that the spectra from atmospheric and marine boundary layers should scale according to variance, wave number and height above the boundary. The spectra from each of the unobstructed runs have been scaled and the results combined to produce the averaged normalized spectra shown in Fig. 7. To calculate the normalized spectra each of the data series was split into two blocks each 512 s long and the autospectra and cospectrum calculated. Each spectrum was then block-averaged, normalized by total variance and scaled by the radian wavenumber $k = 2\pi f/\bar{u}$. The spectra were then averaged to produce estimates equally spaced on a logarithmic frequency scale and ensemble-averaged over the separate runs. The resulting spectra are shown in Fig. 7 plotted against the dimensionless wavenumber $k^* = kz$. The error bars represent ± 1 standard error about the mean and the dashed curves show the average spectral levels found by Soulsby (1977). The high-frequency tail is evident for wavenumbers higher than $\log k^* = 1.2$ which corresponds to a period of about 6.5 s. At shorter wavenumbers the scaled spectra agree reasonably well with those expected from similarity. Soulsby (1977) calculated the total variance by extending the observed spectra over all wavenumbers; the present spectra underestimate the total variance since they only cover a limited range of wavenumber; consequently the scaled results are slightly higher than expected. The results do, in addition, show considerable scatter due to the limited size of the data set. The maxima in the autospectra of u and w, and the uw cospectrum occur, at values of $\log k^*$ equal to -0.4, 0.5 and -0.2; these correspond to time scales of about 200, 30 and 140 s for the energy-containing motions.

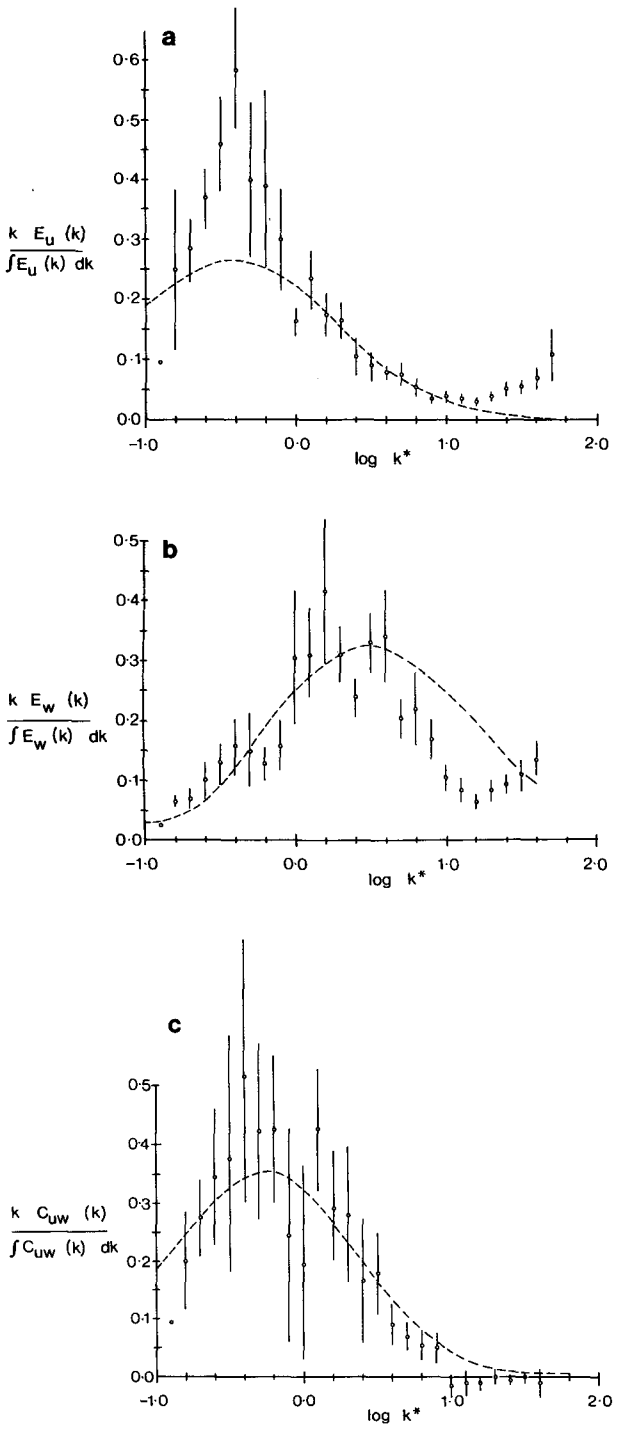

FIG. 7. Ensemble-averaged (a) normalized u spectra, (b) normalized w spectra and (c) normalized uw co-spectra showing the standard errors. The dashed curve is a smoothed representation of the spectrum given by Soulsby (1977).

3. Discussion

The distinctive feature of the turbulence observed in the abyssal boundary layer was its relatively long time scale. The period between bursts of turbulent energy can be estimated from $T_p = 5H/U_\infty$ (Heathershaw, 1979) where H is the thickness of the boundary layer and U_∞ is the free-stream velocity. If we take H as the thickness of an Ekman layer $(0.4u_*/f_c)$ and $U_\infty = 5$ cm s^{-1}, then the burst period is estimated to be around 8 minutes. Alternatively, Blackwelder and Haritonidis (1983) have shown that the burst period is likely to be determined by the near-boundary variables and given by $T_p = 300\nu/u_*$. For the present data this gives a value of about 6 minutes, but the formula is only valid at a nondimensional height of

TABLE 2. High- and low-frequency percentage losses and standard errors (in parentheses) calculated for $U = 5$ cm s^{-1}, $D = 10$ cm and 1 s sampling rate.

Velocity component	High-frequency	Low-frequency 20-minute record	Low-frequency 60-minute record
u^2	4	15 (22)	5 (14)
w^2	15	2 (12)	1 (8)
uw	2	7 (41)	2 (23)

$y^+ = 15$ (where $y^+ = zu_*/\nu$); for the benthic data y^+ has a value of around 400. In spite of this restriction and the uncertainty in the thickness of the boundary layer, both of the above time scales seem to be of the correct magnitude (Fig. 5). Soulsby (1980) has suggested that the digitization rate should not exceed $1.4U/D$ where D is the spatial averaging width; for $U = 5$ cm s^{-1} and $D = 10$ cm this gives a value of 0.7 s^{-1}. The sampling rate is therefore slightly faster than required and no additional information would be obtained by sampling more rapidly. It has been recommended (Soulsby, 1980) that the record length should be sufficiently long that it contains at least 30 bursts so that reliable statistics can be obtained. Figure 5 shows that about 10 events occurred during the 20 minutes and suggests that a one-hour record length would be more appropriate.

The loss of high frequency contributions to the turbulent energy is governed by the sampling rate and the scale of the spatial averaging. For a 1 s sampling rate it is the spatial averaging that is important, and the expected high frequency loss is given in Table 2 (using Fig. 3 from Soulsby, 1980). The low-frequency loss depends on the record length, and has been calculated for records of 20- and 60-minute durations; these results are also given in Table 2. Increasing the record length to 1 hour would improve the low-frequency loss of contributions to uw, reducing it from 7% to 2%. This would be accompanied by a decrease in the standard error from 41% to 23%, giving greater confidence to the stress estimates. Therefore, for future experiments the record length should be increased to one hour. However, if the system samples every 3 hours, as previously, then the capacity of the logger will be exceeded after approximately 3 days. The system should, therefore, be modified to make the sampling conditional on the flow direction so that flow disturbance by the frame can be avoided.

A disappointment of the present system has been the poor agreement found between the two estimates of vertical velocity, w and w' (see Fig. 5). These were measured at points that were separated horizontally by about 50 cm, comparable to the 30 cm length scale found for the horizontal scale of the vertical fluctuations. The lagged correlation between the two signals did not exceed 0.2 even when the flow was aligned with the two heads, and it suggests that the electromagnetic heads need to be closer together before the three-dimensional character of turbulence can be properly evaluated. The agreement found for ratios between the mean flow and the fluctuations when compared with results from shallow water are encouraging, as are the preliminary estimates of the bottom stress. The long time scale associated with turbulent events means that they are adequately resolved by a 1 s sampling rate, and increasing the record length to 60 minutes will reduce the standard error of the stress estimates by 50%.

Acknowledgments. Dr. C. H. Clayson was responsible for the design and construction of much of the electronics, and supervised deployment of the instrument at sea. Mr. A. J. Bunting built the circuits that powered the *e/m* heads. Useful advice and comments were provided by Dr. A. D. Heathershaw and Mr. R. L. Soulsby. The work was undertaken as part of the BENCAT project, of which Dr. S. A. Thorpe was the Project Coordinator.

REFERENCES

Armi, L., and R. C. Millard, 1976: The bottom boundary layer of the deep ocean. *J. Geophys. Res.*, **81**, 4983–4990.

Blackwelder, R. F., and J. H. Haritonidis, 1983: Scaling of the burst frequency in turbulent boundary layers. *J. Fluid Mech.*, **132**, 87–103.

Bowden, K. F., 1962: Measurements of turbulence near the sea bed in a tidal current. *J. Geophys. Res.*, **67**, 3181–3186.

——, and S. R. Ferguson, 1980: Variations with height of the turbulence in a tidally-induced bottom boundary layer. *Marine Turbulence*, J. C. J. Nihoul, Ed., Elsevier, 259–286.

Cartwright, D. E., A. C. Edden, R. Spencer and J. M. Vassie, 1980: The tides of the northeast Atlantic Ocean. *Phil. Trans. Roy. Soc. London*, **A298**, 87–139.

Collar, P. G., and G. Griffiths, 1980: Some comparative studies on electromagnetic sensor heads in laminar and near-turbulent flows in a towing tank. *Oceans '80*, IEEE, 323–329.

D'Asaro, E. A., 1982: Velocity structure of the benthic ocean. *J. Phys. Oceanogr.*, **12**, 313–322.

Elliott, A. J., and S. A. Thorpe, 1983: Benthic observations on the Madeira Abyssal Plain. *Oceanol. Acta*, **6**, 463–466.

Heathershaw, A. D., 1979: The turbulent structure of the bottom boundary layer in a tidal current. *Geophys. J. Roy. Astron. Soc.*, **58**, 395–430.

Richards, K. J., 1984: The interaction between the bottom mixed layer and mesoscale motions of the ocean: A numerical study. *J. Phys. Oceanogr.*, **14**, 754–768.

Saunders, P. M., 1983: Benthic observations on the Madeira Abyssal Plain: Currents and dispersion. *J. Phys. Oceanogr.*, **13**, 1416–1429.

Soulsby, R. L., 1977: Similarity scaling of turbulence spectra in marine and atmospheric boundary layers. *J. Phys. Oceanogr.*, **7**, 934–937.

——, 1980: Selecting record length and digitization rate for near-bed turbulence measurements. *J. Phys. Oceanogr.*, **10**, 208–219.

——, 1983: The bottom boundary layer of self seas. *Physical Oceanography of Coastal and Shelf Seas*, B. Johns, Ed., Elsevier, 189–266.

Weatherly, G. L., and M. Wimbush, 1980: Near-bottom speed and temperature observations on the Blake–Bahama Outer Ridge. *J. Geophys. Res.*, **85**, 3971–3981.

Wimbush, M., and W. Munk, 1970: The benthic boundary layer. *The Sea*, Vol. 4, A. E. Maxwell, Ed., Wiley–Interscience, 731–758.